Synthesis, Antiproliferative and Antimalarial Activities of Dinuclear Silver(I) Complexes with Triphenylphosphine and Thiosemicarbazones Ligands

Nur Adila Fatin Mohd Khir[1], Mohd Ridzuan Mohd Abd Razak[2], Fariza Juliana Nordin[3], Nur Rahimah Fitrah Mohd Sofyan[1], Nor Fadilah Rajab[3], and Rozie Sarip[1*]

[1]*Department of Chemistry, Faculty of Science, University of Malaya (UM), Lembah Pantai, 50603 Kuala Lumpur, Malaysia*

[2]*Bioassay Unit, Herbal Medicine Research Centre (HMRC), Institute for Medical Research (IMR), Jl. Pahang, 50588 Kuala Lumpur, Malaysia*

[3]*Faculty of Health Sciences, Universiti Kebangsaan Malaysia (UKM), Kuala Lumpur Campus, Jl. Raja Muda Abdul Aziz, 50300 Kuala Lumpur, Malaysia*

Abstract: *A series of six sulfur-bridged dinuclear silver(I) thiosemicarbazone complexes were synthesized through the reaction of silver(I) nitrate with 4-phenyl-3-thiosemicarbazone derivatives together with triphenylphosphine (PPh₃) (in a 1:1:2 molar ratio). Following structural characterizations using various techniques such as elemental analysis, Fourier-transform infrared (FTIR) spectroscopy, as well as ^1H, ^{13}C, $^{31}P\{^1H\}s$, COSY, and ^1H-^{13}C nuclear magnetic resonance (NMR) spectroscopy, it was found that the thiosemicarbazone ligand exists in the form of a thione rather than thiol tautomer. Subsequently, MDA-MB-231 and MCF-7 breast cancer cell lines, as well as the HT-29 colon cancer cell lines, were used to investigate the in vitro antiproliferative activities of these complexes. In all cases, the IC_{50} values were in the potent micromolar range. Besides, the aforementioned complexes also had good antiplasmodial activity against chloroquine-resistant* P. falciparum*, as per the results of histidine-rich protein 2 (HRP2) assays and cytotoxicity evaluations of MDBK cells.*

Keywords: *thiosemicarbazone; silver complexes; antiplasmodial; antiproliferative; phosphine*

■ INTRODUCTION

The synthesis of metal complexes containing mixed ligand systems that have electron-donating potential has attracted much attention owing to their catalytic abilities [1], unique structures [2], and most importantly, applications in the medical field [3-4]. In particular, metal complexes with phosphine and thiosemicarbazone ligands have been explored due to the ability of thiosemicarbazone to coordinate a wide range of metallic ions that can be attributed to the extended delocalization of the electron density of the NH-CS-NH-N system [5]. The employment of transition metals in drug discovery has become a favorite approach, especially when it is attached to compounds of common therapeutic value like thiosemicarbazones in an effort to fight drug resistance

[6]. In addition, metal coordination also helps to increase the lipophilicity of a compound, hence increasing the speed of the compound's entry into the cell [7].

Research interest in these compounds is also fueled by their broad spectrum of biological activities, including antibacterial [8], antiviral [9], antitubercular [10], and antitumor [11], anticancer and antimalarial activities [5]. Evidently, silver complexes and their therapeutic abilities are interesting topics among researchers [12]. A previous study combining the ligands of thio and phosphine has shown a promising activity towards antibacterial activity [13]. Another study used a similar group of ligands (thio and phosphine), but gold also showed higher cytotoxicity, better antitumor activity,

and selectivity than the cisplatin [14]. However, to the ability of our knowledge, there is a lacking recent report on the screening for the anticancer potential and the antiplasmodial properties of the silver(I) complexes with thiosemicarbazone and triphenylphosphine ligands.

Hence, as a part of continuing interest in this area of research, we synthesized a series of thiosemicarbazone-derivative ligands, which were then attached to a silver center along with triphenylphosphine ligands. The silver complexes were later characterized using few elemental and spectral analyses to confirm their structure. Basic elemental analysis like CHNS and PXRD was used to confirm the composition and types of elements present in the complexes. Afterward, more detailed spectroscopy techniques like FTIR, 1D NMR, and 2D NMR were used to justify the structure of the complexes.

■ EXPERIMENTAL SECTION

Materials

Chemicals of 4-nitrobenzaldehyde, 4-hydroxy benzaldehyde, 5-bromosalicylaldehyde, 5-bromoindole-3-carboxaldehyde (98%, Sigma Aldrich), 2-methylindole-3-carboxaldehyde, (5-bromo-2-hydroxy-3-methoxy benzaldehyde (97%, Sigma Aldrich), triphenylphosphine, 4-phenyl thiosemicarbazide (99%, Sigma Aldrich) were used in this study. All reagents and solvents used were of reagent grade without prior purification unless otherwise stated. The progress of these reactions was observed via thin-layer chromatography performed on 2.00×6.00 cm aluminium sheets pre-coated with silica gel 60 (HF-254, Merck) of thickness 0.25 mm.

Instrumentation

The Fourier-transform infrared (FTIR) spectra were recorded by a Perkin Elmer Spectrum One FT-IR spectrophotometer (ATR) at 450–4000 cm^{-1}. The ^1H, ^{13}C, $^{31}P\{^1H\}$, COSY, and ^1H-^{13}C nuclear magnetic resonance (NMR) spectra were analyzed using a JEOL FT-NMR ECX 400 (ECX 400) spectrometer, whereby deuterated dimethyl sulfoxide (DMSO) and chloroform were the solvents. Meanwhile, Perkin Elmer CHNS/O Analyzer 2400 Series II was used to perform the elemental analyses, while Energy Dispersive X-Ray spectroscopy (EDX) was

used to detect the presence of silver metal. X-ray diffractometer (PANalytical, Netherlands) was used to examine Powder X-ray diffraction (PXRD) with a scanning scope of 2θ from 0 to 50° and scanning rate of 4.25°/min at room temperature (25 °C), with Cu Kα characteristic radiation (λ = 0.154 nm) at the current of 40 mA and voltage of 40 kV.

Procedure

Synthesis of thiosemicarbazone ligands (L1-L6)

All thiosemicarbazone ligands (**L1**-**L6**) were prepared by the procedure described in Ref. [15], with slight modifications (Scheme 1). First, 4-phenyl-3-thiosemicarbazide (1 g, 6 mmol) was dissolved in ethanol (33 mL). Next, the corresponding aldehyde (which was pre-dissolved in ethanol) was added to the mixture along with a few small drops of glacial acetic acid. The solution was then refluxed for 3–4 h and later dried in a vacuum for analysis. The ligands were white or yellow powders soluble in ethanol, methanol, acetone, DMSO, dichloromethane, or chloroform.

L1: 4-nitrobenzaldehyde-N-phenyl-thiosemicarbazone. Yield: 70%, M.p. 260 °C. Anal. Calc. for $C_{14}H_{12}N_4O_2S$: C, 56.00; H, 4.02; N, 18.63. Found: C, 55.20; H, 3.73; N, 18.59. IR data (cm^{-1}): (N–H) 3103.08, 2980.20,
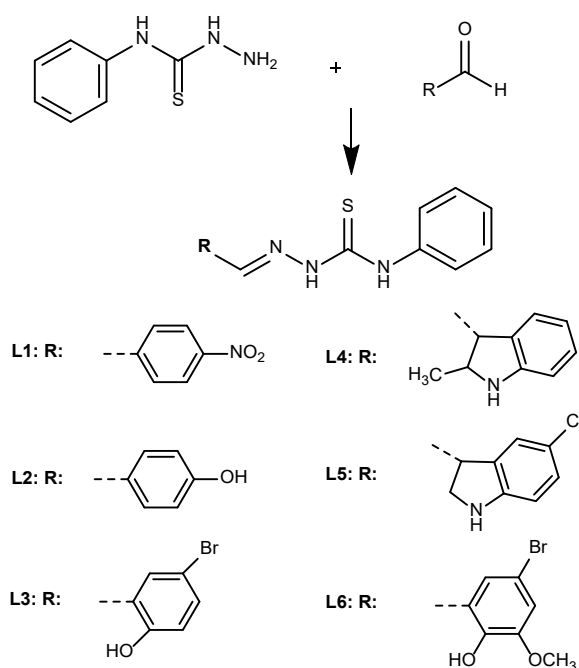
Scheme 1. Synthesis of thiosemicarbazone ligands

(C=N) 1595.02, (C=S) 846.76, ¹H-NMR data (δ, ppm; DMSO): 12.06 (s, 1H) (N–H), 10.29 (s, 1H) (N–H), 8.20 (C–H, 1H) (CH=N), 7.2–8.2 (m) (CH, CH₂, CH₃); ¹³C-NMR data (δ, ppm; DMSO): 177.10 (C=S), 140.70 (C-Ph).

L2: 4-hydroxybenzaldehyde-N-phenyl-thiosemicarbazone. Yield: 60%, M.p. 240 °C. Anal. Calc. for $C_{14}H_{13}N_3OS$: C, 61.97; H, 4.83; N, 15.49. Found: C, 61.24; H, 4.92; N, 14.98. IR data (cm⁻¹): (N–H) 3158.08, 2977.11 (C=N) 1604.28 (C=S) 851.49, ¹H-NMR data (δ, ppm; DMSO): 11.62 (s, 1H) (N–H), 9.94 (s, 1H) (N–H), 9.88 (s, 1H) (C–OH), 8.04 (s, 1H) (CH=N), 6.8–8.1 (m) (CH, CH2, CH₃); ¹³C-NMR data (δ, ppm; DMSO): 175.90 (C=S), 144.00 (C-Ph).

L3: 5-bromo-2-hydroxybenzaldehyde-N-phenyl-thio semicarbazone. Yield: 65%, M.p. 250 °C. Anal. Calc. for $C_{14}H_{12}BrN_3OS$: C, 48.01; H, 3.45; N, 12.00. Found: C, 48.24; H, 3.44; N, 12.12. IR data (cm⁻¹): (N–H) 3141.28, 2984.50 (C=N) 1604.57 (C=S) 829.04, ¹H-NMR data (δ, ppm; DMSO): 11.78 (s, 1H) (N–H), 10.14 (s, 1H) (N–H), 10.28 (s, 1H) (C–OH), 8.38 (s, 1H) (CH=N), 6.7–7.5 (m) (CH, CH2, CH₃); ¹³C-NMR data (δ, ppm; DMSO): 176.60 (C=S), 139.50 (C-Ph).

L4: 2-methylindole-3-carboxaldehyde-N-phenyl-thio semicarbazone. Yield: 80%, M.p. 230 °C. Anal. Calc. for $C_{17}H_{16}N_4S$: C, 65.78; H, 5.84; N, 18.05. Found: C, 66.01; H, 5.19; N, 17.32. IR data (cm⁻¹): (N–H) 3394.64, 3285.30. 3209.93, (C=N) 1589.25 (C=S) 839.31, ¹H-NMR data (δ, ppm; DMSO): 11.55 (s, 1H) (N–H_indole); 11.40 (s, 1H) (N–H), 9.50 (s, 1H) (N–H), 8.50 (s, 1H) (CH=N), 6.7–7.0 (m) (CH, CH₂, CH₃); ¹³C-NMR data (δ, ppm; DMSO): 174.50 (C=S), 141.70 (C-Ph).

L5: 5-chloroindole-3-carboxaldehde-N-phenyl-thio semicarbazone. Yield: 45%, M.p. 210 °C. Anal. Calc. for $C_{16}H_{15}ClN_4S$: C, 58.09; H, 4.57; N, 16.93. Found: C, 57.65; H, 3.95; N, 16.20. IR data (cm⁻¹) : (N–H) 3338.98, 3132.20, 2973.42 (C=N) 1609.25 (C=S) 866.50, ¹H-NMR data (δ, ppm; DMSO): 11.83 (s, 1H) (N–H), 11.58 (s, 1H) (N–H_indole), 9.72 (s, 1H) (N–H), 8.35 (s, 1H) (CH=N), 7.0–8.2 (m) (CH, CH₂, CH₃) ¹³C-NMR data (δ, ppm; DMSO): 175.10 (C=S), 141.20 (C-Ph).

L6: 5-bromo-2-hydroxy-3-methoxybenzaldehyde-N-phenyl-thiosemicarbazone. Yield: 70%, M.p. 190 °C. Anal. Calc. for $C_{15}H_{14}BrN_3O_2S$: C, 47.38; H, 3.71; N, 11.05.

Found: C, 47.89; H, 3.75; N, 11.08. IR data (cm⁻¹): (N–H) 3300.41, 2973.79 (C=N) 1604.00, (C=S) 858.86. 1H-NMR data (δ, ppm; DMSO): 11.80 (s, 1H) (N–H), 10.10 (s, 1H) (N–H), 9.49 (s, 1H) (OH), 8.43 (s, 1H) (CH=N), 3.81 (s, 1H) (OCH₃), 7.0–7.6 (m) (CH, CH2, CH3); ¹³C-NMR data (δ, ppm; DMSO): 176.60 (C=S), 140.00 (C-Ph).

Synthesis of complexes (P1-P6)

AgNO₃ (0.17 g, 1 mmol) was first dissolved in a 20 mL mixture of acetonitrile and methanol (2:3), following which the respective thiosemicarbazone ligands (**L1**-**L6**) (2 mmol) were added. The mixture was refluxed at 55 °C for 3–4 h. The mixture was further added with triphenylphosphine (0.262 g, 1 mmol) in 5 mL of acetonitrile/methanol (2:3) and further refluxed for 2–3 more hours. The latter step could result in the solubilization of the precipitates obtained in the first step, if any. Thin-layer chromatography is used to monitor the reaction's progress. The resulting solution was filtered and later thoroughly dried via evaporation. Further purification was performed before the analysis. The silver complexes were brown and black powders and soluble in either DMSO or a mixture of methanol and acetonitrile.

P1: [Ag₂(PPh₃)₂(L1)₄]·(NO₃)₂·H₂O. Yield: 50%, M.p. 157–160 °C. Anal. Calc. for $C_{92}H_{78}Ag_2N_{16}O_8P_2S_4$ C, 56.91; H, 4.05; N, 11.54; S, 6.61. Found: C, 56.30; H, 3.57; N, 11.65; S, 6.61. IR data (cm⁻¹): (N–H) 2983.12, 2888.57, (C=N) 1589.21 (C=S) 840.88. ¹H-NMR data (δ, ppm; DMSO): 12.33 (s, 4H) (N–H), 10.72 (s, 4H) (N–H), 8.18 (C–H, 4H) (CH=N), 7.1–8.3 (m) (CH, CH₂, CH₃). ¹³C-NMR data (δ, ppm; DMSO): 175.80 (C=S), 143.00 (C-Ph).

P2: [Ag₂(PPh₃)₂(L2)₄]·(NO₃)₂·H₂O. Yield: 45%, M.p. 135–138 °C.); Anal. Calc. for $C_{92}H_{82}Ag_2N_{12}O_4P_2S_4$ C, 60.53; H, 4.53; N, 9.21; S, 7.03. Found: C, 58.90; H, 3.82; N, 9.26; S, 6.48. IR data (cm⁻¹): (N–H) 2981.06, 2889.37 (C=N) 1595.67, (C=S) 834.24. ¹H-NMR data (δ, ppm; DMSO): 11.88 (s, 4H) (N–H), 10.22 (s, 4H) (N–H), 7.99 (s, 4H) (CH=N), 9.98 (s, 4H) (O–H), 6.6–7.5 (m) (CH, CH2, CH3) ; ¹³C-NMR data (δ, ppm; DMSO): 173.90 (C=S), 146.60 (C-Ph).

P3: [Ag₂(PPh₃)₂(L3)₄]·(NO₃)₂·H₂O. Yield: 40%. M.p. 140–143 °C. Anal. Calc. for: $C_{92}H_{78}Ag_2Br_4N_{12}O_4P_2S_4$ C, 51.60; H, 3.67; N, 7.85; S, 5.99. Found: C, 49.65; H, 3.17; N, 7.81; S, 5.31. IR data (cm⁻¹): (N–H) 3141.28, 2984.50 (C=N) 1604.57, (C=S) 824.43. ¹H-NMR data (δ, ppm; DMSO): 12.02 (s, 4H) (N–H), 10.46 (s, 4H) (N–H), 8.42 (s, 4H) (CH=N), 10.58 (s, 4H) (O–H) 6.8–7.5 (m) (CH, CH2, CH3); ¹³C-NMR data (δ, ppm; DMSO): 174.00 (C=S), 141.50 (C-Ph).

P4: [Ag₂(PPh₃)₂(L4)₄]·(NO₃)₂·H₂O. Yield: 45%. M.p. 127–130 °C. Anal. Calc. for $C_{104}H_{94}Ag_2N_{16}P_2S_4$ C, 63.28; H, 4.80; N, 11.35; S, 6.50. Found: C, 59.62; H, 4.34; N, 10.98; S, 5.89. IR data (cm⁻¹): (N–H) 3012.28, 2880.97, 2649.02 (C=N) 1600.00 (C=S) 830.01. ¹H-NMR data (δ, ppm; DMSO): 11.63 (s, 1H) (N–H$_{indole}$), 11.60 (s, 4H) (N–H), 9.73 (s, 4H) (N–H), 8.41 (s, 4H) (CH=N), 7–7.5 (m) (CH, CH2, CH3). ¹³C-NMR data (δ, ppm; DMSO): 172.90 (C=S), 144.00 (C-Ph).

P5: [Ag₂(PPh₃)₂(L5)₄]·(NO₃)₂·H₂O. Yield: 40%. M.p 131–134 °C. Anal. Calc for $C_{100}H_{86}Ag_2N_{16}P_2S_4$ C, 62.63; H, 4.52; N, 11.69; S, 6.69 Found: C, 59.89; H, 3.89; N, 10.91; S, 6.53. IR data (cm⁻¹): (N–H) 3000.96, 2883.01, 2733.51, (C=N) 1598.27, (C=S) 834.04. ¹H-NMR data (δ, ppm; DMSO): 11.88 (s, 1H) (N–H$_{indole}$), 10.35 (s, 4H) (N–H), 10.01 (s, 4H) (N–H), 8.00 (s, 4H) (CH=N), 6.8–7.8 (m) (CH, CH2, CH3). ¹³C-NMR data (δ, ppm; DMSO): 173.70 (C=S), 133.80 (C-Ph).

P6: [Ag₂(PPh₃)₂(L6)₄]·(NO₃)₂·H₂O. Yield: 40%. M.p 137–140 °C. Anal. Calc for $C_{96}H_{86}Ag_2Br_4N_{12}O_8P_2S_4$ C, 50.99; H, 3.83; N, 7.43; S, 5.67. Found: C, 48.09; H, 3.38; N, 7.72; S, 6.02. IR data (cm⁻¹): (N–H) 3049.11, 2879.23, (C=N) 1599.12 (C=S) 742.69. ¹H-NMR data (δ, ppm; DMSO): 12.00 (s, 4H) (N–H), 10.53 (s, 4H) (N–H), 8.46 (s, 4H) (CH=N), 9.52 (s, 4H) (O–H), 7.0–7.4 (m) (CH, CH2, CH3). ¹³C-NMR data (δ, ppm; DMSO): 174.40 (C=S), 836.84 (C-Ph)

Biological procedures

Antiplasmodial assays. The antiplasmodial activities of all compounds were evaluated *in vitro* through HRP2 assays [16-17] as described in Ref. [18] with some alterations. First, the compounds were solubilized in 100% DMSO and serially diluted into mixtures whose concentrations range from 25 μM to 0.39 μM in wells A1

to A7 of a 96-well plate. Some 15 μL of each serially-diluted stock extract was moved accordingly into plates with 225 μL of sterile H₂O. Aliquots from the plates would be used in the HRP2 assays. Next, ring-infected red blood cells (RBCs) of 5% parasitemia were tuned so that the parasitemia and hematocrit were 0.05% and 1.5%, respectively. Ten μL of each serially-diluted extract was moved to a test plate containing parasitized RBCs and later incubated in a candle jar at 37 °C for 72 h. The final test concentrations ranged from 0.156 μM to 0.002 μM, while DMSO was 0.3%. Artemisinin (Art) (Sigma, USA), chloroquine (CQ) (Sigma, USA), mefloquine (Mef) (Sigma, USA), and quinine (Q) (Sigma, USA) – whose final test concentrations were 1772.6–27.7 nM for CQ, 3495–54.6 nM for Q, 601.3–9.4 nM for Mef, and 51.2–0.8 nM for Art – were the standard controls used to validate the test. Meanwhile, the negative controls comprised infected RBCs without extracts or with sterile H₂O only. Following incubation for 72 h, the test plates were then kept overnight at -80 °C. It was then thawed at room temperature to lyse the infected RBCs. Subsequently, the activities of the compounds against the parasite were measured via HRP2 assays [17,19].

Cytotoxicity assays (in vitro). The MDBK cells were preserved in complete Dulbecco's Modified Eagle Medium (DMEM) comprising 25 mM 4-(2-hydroxyethyl)-1-piperazineethanesulfonic acid (HEPES), 100 U of Pen-strep (100 U penicillin and 100 U streptomycin), 0.4% sodium bicarbonate (NaHCO₃) accompanied with 10% fetal bovine serum (FBS). 3-(4,5-dimethylthiazol-2-yl)-2,5-diphenyltetrazolium bromide (MTT) assays were used to test the cytotoxicities of the extracts [20]. Briefly, MDBK cells (1×10^3 cells/well) which have been cultured overnight were exposed to serially diluted (2-fold-diluted) compounds whose final concentrations ranged from 0.25 μM to 0.004 μM. The final concentrations of DMSO in all tests were less than 1%. All tests were performed in duplicates. Cell suspension lacking the test material was the positive control for cell growth, while the negative control cell contains suspension with 0.05% Triton X 100. The test culture was kept for 72 h at 37 °C in a 5% CO₂ incubator. To each well, some 50 μL of MTT solution (2.5 mL

DMEM and 5 mg MTT in 1 mL PBS) were added. It was then kept for 4 h at 37 °C in the said incubator. Next, the medium was removed and replaced with 200 μL of DMSO to solubilize the MTT formazan product. It was then mixed for 15 min before its absorbance was measured using a microplate reader (FLUOstar Omega, Germany) at 540 nm. The IC_{50} and growth inhibition percentage were predicted with reference to a dose-response curve.

Antiproliferative assays. Sulforhodamine B (SRB) assays were performed to determine the IC_{50} of the test compounds as described in previous studies [21]. Briefly, the cells were treated with 5.053–161.686 μM, 4.843–154.960 μM, 4.189–134.055 μM, 4.680–149.752 μM, or 3.936–125.944 μM sets of concentrations for all the synthesized complexes. Forty-eight hours later, using 50 μL of 50% (w/v) trichloroacetic acid (TCA), the cells were secured to the plates and kept further incubated at 4 °C for an hour. The plates were then washed five times using tap water, air-dried, stained with 100 μL of 0.4% (w/v) SRB staining solution, and further incubated for another 10 min at room temperature. Consequently, the plates were washed three times with 1% (v/v) acetic acid to remove the unbound stains. Following air-drying, 200 μL of 10 mM Trizma base was added into the wells, shaken for 10 min. The reading of the absorbance is taken using a microplate reader at 490 nm, and the IC_{50} calculated using the formula; IC_{50} = (OD sample/OD control) × 100. All experiments were performed in triplicates.

■ RESULTS AND DISCUSSION

The six silver(I) complexes which were synthesized in a molar ratio of 1:1:2 (Ag:PPh₃:thiosemicarbazone) were either brown and black, were structurally characterized by nuclear magnetic resonance (NMR), Fourier-transform infrared (FTIR) spectroscopy, energy-dispersive X-ray (EDX), powder X-ray diffraction (PXRD), and elemental analysis. The spectroscopic data interpreted that all the ligands and their corresponding complexes existed in the form of thione tautomers. The formation of silver complexes occurred when silver received a lone pair of electrons from donor sulfur and phosphorus atoms. These complexes were believed to bind tightly to the metal center through M-S bridging

bonds as they were synthesized in a molar ratio of 1:1:2 [22]. In agreement with the results of previous studies [22-23], the silver complexes were dinuclear, with each silver atom tetrahedrally coordinated to one S atom with a thiosemicarbazone terminal, and two S atoms with a bridging thiosemicarbazone group, and one P atom of triphenylphosphine (PPh₃) as shown in Fig. 1.

Fourier-Transform Infrared Spectroscopy (FTIR)

To investigate the points of attachment of the ligands to the metal center in the complexes, the FTIR spectra of the free ligands were compared to its synthesized complexes. The infrared spectra of the corresponding complexes confirmed the coordination of the ligand as $\upsilon(C=N)$ vibrational modes were detected in all of the ligands and complexes. The shifting of the $\upsilon(C=S)$ bands to lower energies in the complexes meant that the thiosemicarbazone ligands were coordinated to the silver (I) metal via donor sulfur atoms. Meanwhile, the absence of $\upsilon(S–H)$ bands at the 2800–2550 cm⁻¹ regions of both ligands and complexes revealed that the
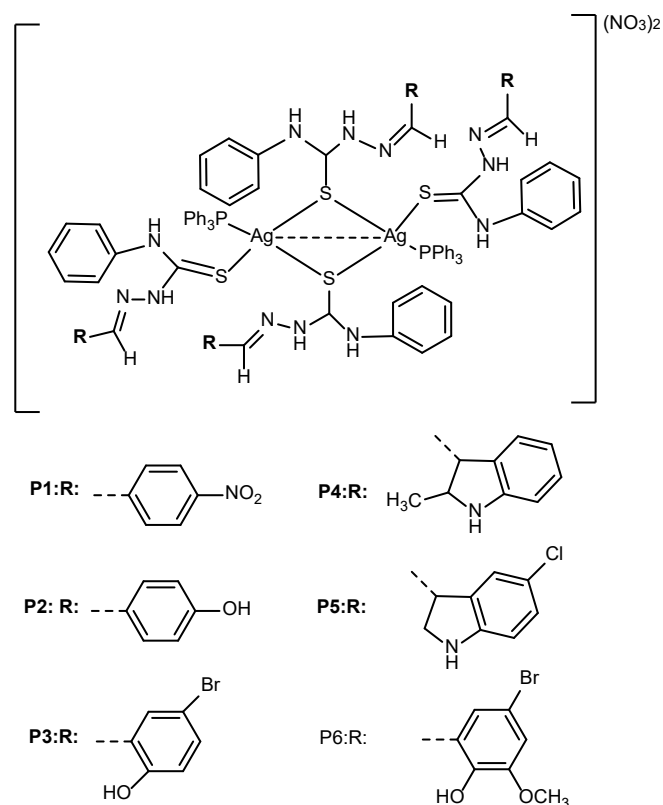
Fig 1. Structures of the silver complexes **P1**–**P6**

complexes only had thione tautomers which were retained from their free ligands. Intra- and inter-molecular hydrogen bonds of the hydroxyl and amino groups, which gave rise to band-broadening in the 3500–3000 cm^{-1} regions, were also present. A characteristic υ(P–C$_{Ar}$) peak at around 1090 cm^{-1} denoted the presence of triphenylphosphine that was coordinated to the silver center. A sharp band around 1300 cm^{-1} was detected in all complexes, suggesting non-coordinated NO$_3^-$ ions. However, the FTIR spectrum of **P5** did not reveal a –C–Cl peak, unlike that of its ligand (**L5**). This occurrence further proposed the detachment of –Cl to form HCl in the reaction mixture.

Nuclear Magnetic Resonance (NMR) Spectroscopy

In the ^{1}H-NMR spectra of the complexes, signals from the aromatic protons were confirmed by the presence of multiplet peaks observed at 6.00–8.00 ppm. Concurrently, following coordination with silver metal, the N–H signals from the metal complexes were shifted downfield by around 0.20–0.50 ppm from their original positions in the free ligands (δ = 9.5–12.0 ppm). As for

compounds **P2**, **P3**, and **P6**, the hydroxyl proton peaks at δ = 9.98, 10.58, and 9.70 ppm were also shifted slightly downfield. On the same note, **P6** also gave rise to a methoxy-proton peak in the form of a triplet at δ = 3.80 ppm. The coordination of the triphenylphosphine ligand was evidenced by the presence of additional aromatic protons at δ = 7.10–7.50 ppm in the complexes; these were not otherwise present in their respective ligands. Fig. 2 shows the assignments of protons in the ^{1}H-NMR spectrum of compounds **4**.

In the ^{13}C-NMR spectra, the bonding between the thiosemicarbazone and phosphine ligands to the metal centers was also proven by the presence of C=S signals in which the chemical shift value was around 2.0 ppm. This was in view of the decrease of the C=S bond when attached to metal [24], as well as a shift in the N→C electron density, which gave rise to a partial bond characteristic in the C–N bond [25]. With reference to compounds **P2**, **P3**, and **P6**, the C-hydroxyl resonance at the thiosemicarbazone ligand was observed at δ = 139.00 ppm. In further detail, the spectrum for the
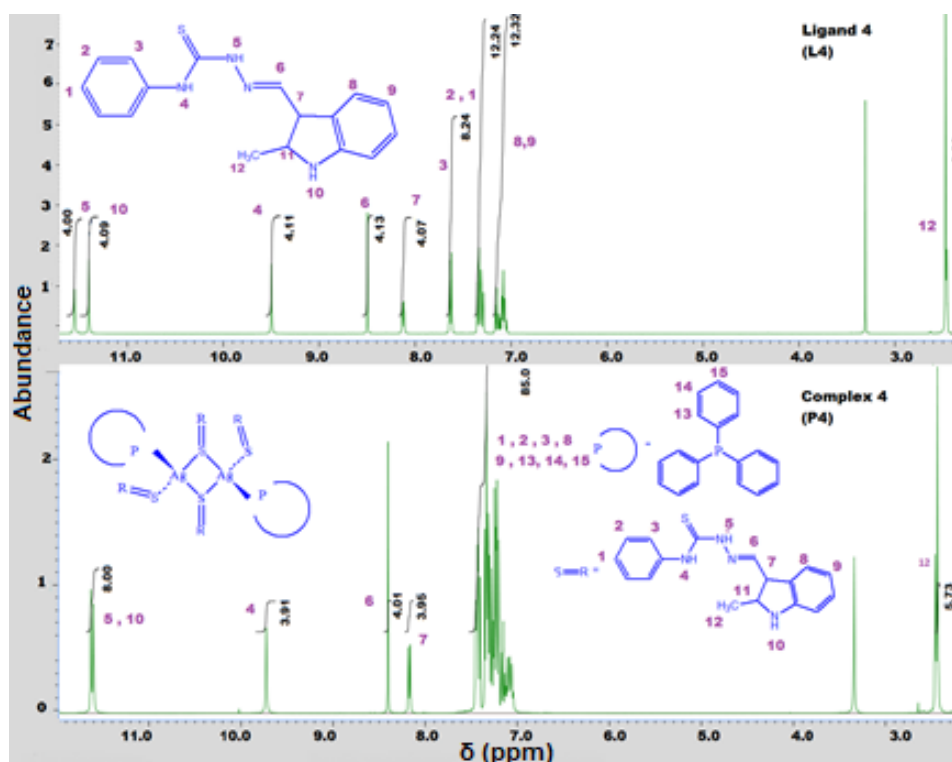
Fig 2. ^{1}H-NMR spectra of compounds **L4** and **P4**

compound **P6** had a C-methoxy resonance at δ = 57.0 ppm, while the C-methyl resonance in compound **P4** was observed at δ = 12.0 ppm. In all complexes, the resonances of the aromatic carbons in triphenylphosphine and thiosemicarbazone revealed significant upfield shifts at δ = 131.0–132.0 ppm. Since the aromatic C on triphenylphosphine appeared as doublets and singlet, these further confirmed the attachment of the triphenylphosphine ligand to the silver center [25]. Fig. 3 shows the assignments of carbon peaks for the ligand and complex **4**.

The ¹H-¹H COSY NMR has further authenticated the correlation between the equivalent proton pairs with the adjacent protons wherein the cross peak resulting from the correlation appears in the same region. Fig. 4 shows the COSY spectrum for complexes **P3**. From the figure, the proton H5 is correlated to the proton H4 and H6. Meanwhile, H10 is correlated to the aromatic proton area near 7 ppm. A similar phenomenon can also be found by H7 which correlates with the aromatic proton area near 7 ppm while the H8 correlates to the aromatic
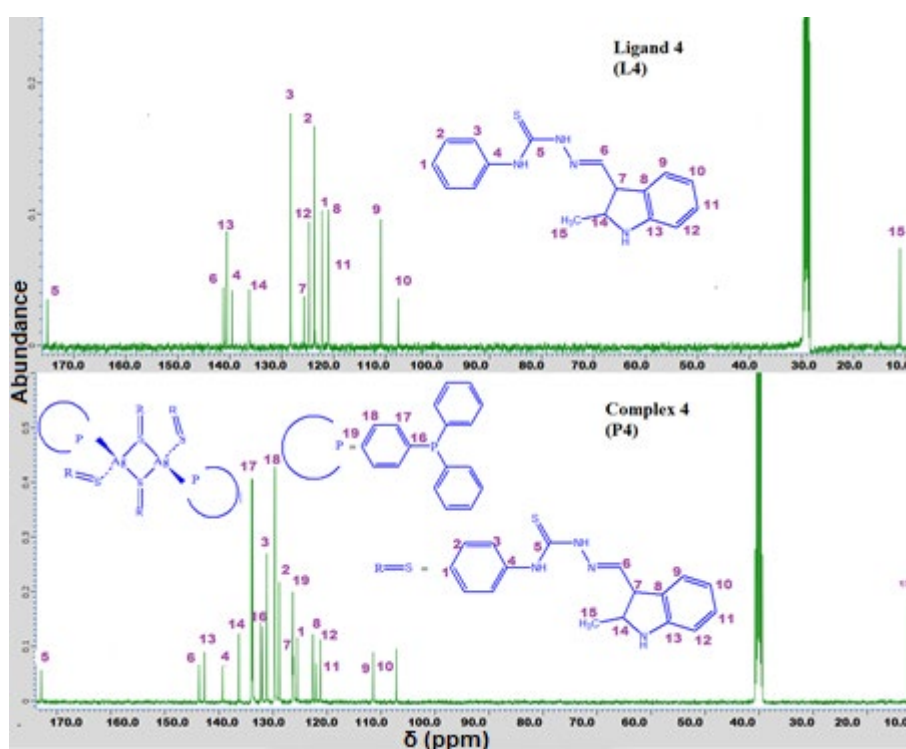
Fig 3. ¹³C-NMR spectra of **L4** and **P4**
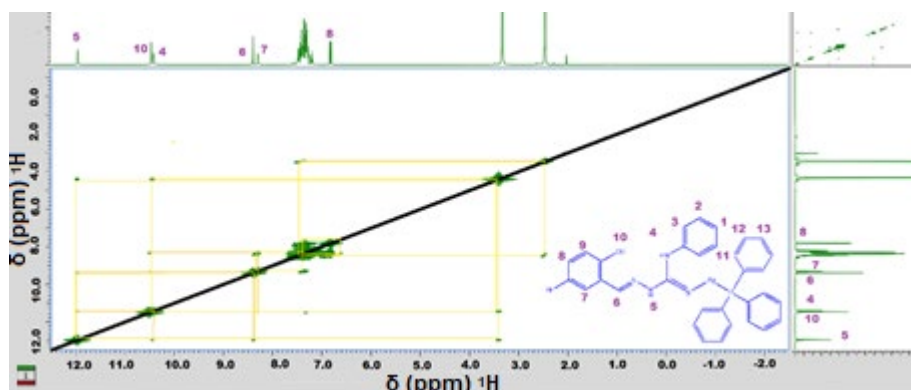
Fig 4. COSY NMR spectrum of complexes **P3**

proton peak indisputably H9. The COSY spectra also reveal that the H10 adjacent to the O atom in the hydroxyl group and H5 connected to the N atom is correlated with the H_2O peak from the deuterated DMSO.

The ^1H–^{13}C HSQC spectra of compounds demonstrate the interaction between the protons and the carbon atoms which are attached. As a representative, the discussion will be based on the spectrum for ligand and complex **P6** (Fig. 5). It can be deduced from Fig. 2 that the H6 is correlated with C6. A similar phenomenon can also be found on the H8, which relates to C10 as justified in the structure numbering shown in the figure. The aromatic carbons in the compound were established via the connectivities between the carbon and its neighboring proton by HSQC correlation spectra. H1, H2, H3, H11, H12, H13, and H7 in the aromatic ring are correlated with C1, C2, C3, C14, C15, C16, and C8, respectively.

In the $^{31}P\{^1H\}$-NMR spectra of complexes **P1** to **P6**, a sharp singlet was observed at $\delta = 10.0$ ppm. This result suggested that the resonance of phosphorus in triphenylphosphine has shifted downfield as compared to that of its free ligand [13] ($\delta = -5.5$ ppm). In other words, complexation occurred between the silver center and the triphenylphosphine ligand. Fig. 6 shows the ^{31}P-NMR spectra of triphenylphosphine and silver complex **P4**.

Powder X-Ray Diffraction (PXRD) Analysis

To produce sufficient crystals for single-crystal X-ray analyses, the crystals of all synthesized complexes were grown several times using various methods, including those of previous studies that have managed to generate single crystals [22-26]. Some of these methods included slow evaporation at room temperature and low temperature (refrigerator) for several days, as well as recrystallization of the products scraped from organic solvents (DMF, DMSO, acetonitrile, methanol). However, crystals were not successfully grown that can be further used for X-ray diffraction studies. According to Altaf et al., silver compounds whose ligands contained
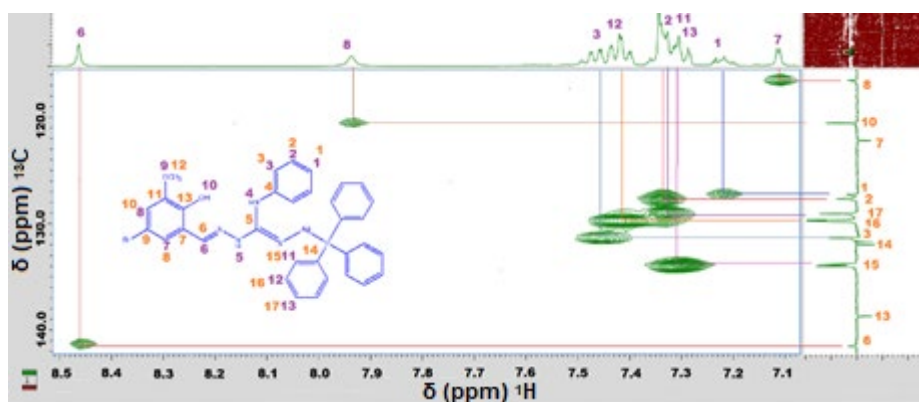
Fig 5. HSQC spectrum for complexes **P6**
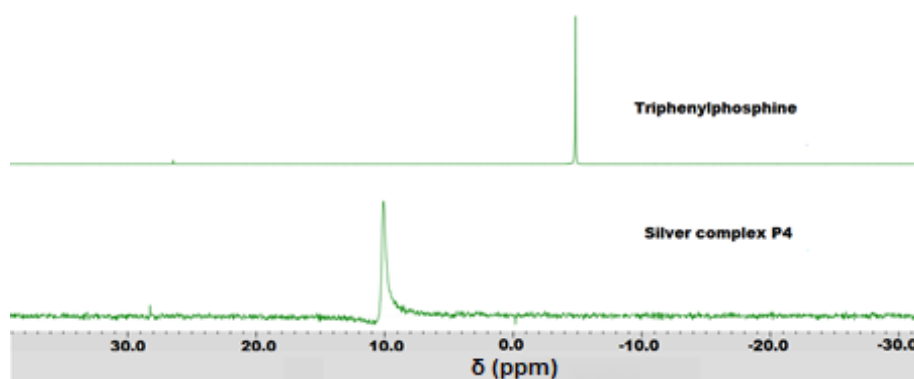
Fig 6. $^{31}P\{^1H\}C$-NMR spectra of free ligand (triphenylphosphine) and silver complex

nitrogen and sulfur were hard to crystallize owing to their tendency to form intramolecular interactions and polymeric states [22]. Thus, we probed the complexes via PXRD analysis to determine their phases, unit cell dimensions, as well as sample purities. Fig. 7 shows the PXRD pattern for compound **5** (**L5** and **P5**). All other diffractograms can be found in Supplementary Information associated with this report. The PXRD diffractograms were taken within 2θ ranges of 5–40°. The observed broad peaks were attributed to the non-crystalline samples.

Energy Dispersive X-ray (EDX) Spectroscopy

EDX spectroscopy was also conducted to verify the existence of silver metal in all complexes (see Supplementary Information). Based on the results of the analyses, silver metal was present in all six series of

complexes. Other elements such as carbon, nitrogen, oxygen, sulfur, phosphorus, and bromine, which were expected to be present in the ligands, were also present in the complexes.

Antiplasmodial Study

All complexes demonstrate suitable antiplasmodial activities in the *in vitro P. falciparum* HRP2 assays against chloroquine-resistant *P. falciparum* parasites (in the asexual cycle) in red blood cells (Table 1). All silver complexes (except **P1**) were tested for this study. The cytotoxic activity of the compounds on MDBK cells was evaluated in terms of the proportion of cytotoxicity to biological activity (SI). The biological efficacy was not attributable to *in vitro* cytotoxicity when the index was ≥ 10 [27]. However, the compounds better inhibited the growths of normal cell lines, MDBK cells,
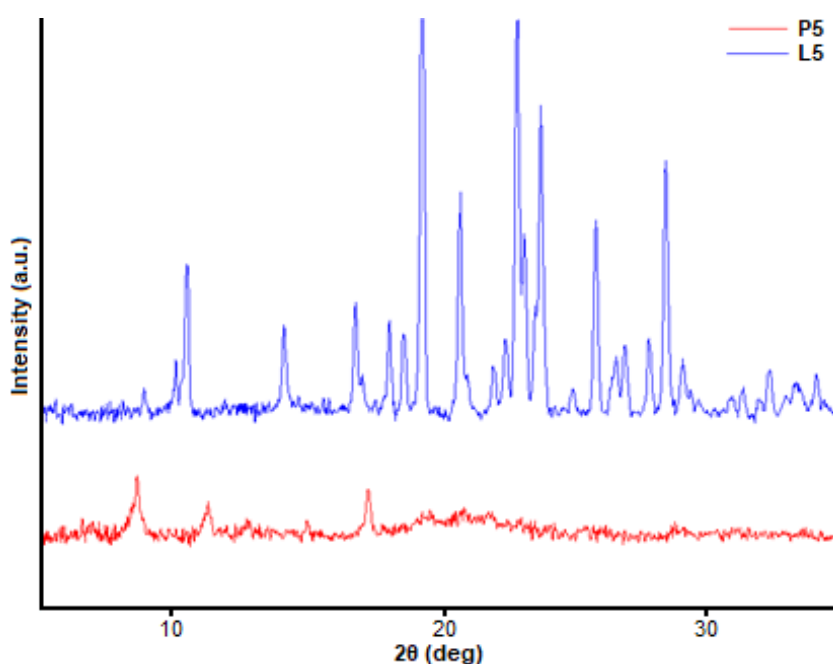
Fig 7. PXRD diffractograms of ligand and complex **P5**

Table 1. Antiplasmodial and cytotoxicity activity of silver complexes **1-6** (EC50 in μM)

Complexes	*P. falciparum* HRP2	Normal MDBK	Selectivity Index (SI)
P1	-	-	-
P2	1.739 ± 0.243	1.215± 0.180	0.699
P3	4.000 ± 0.142	0.821 ± 0.068	0.205
P4	2.120 ± 1.184	0.945 ± 0.102	0.446
P5	3.776 ± 0.280	0.984 ± 0.046	0.261
P6	4.266 ± 0.311	1.675 ± 0.183	0.393

than *P. falciparum* (Table 1). Specifically, the SI of each compound was less than 10, thereby suggesting that the antiplasmodial activities of the compounds could be due to *in vitro* cytotoxicity.

Concerning the selectivity indices of silver complexes, **P2** had the highest SI (0.699) while **P3** the lowest (0.205). This could be explained by the existence of a hydroxyl group at the *-para* position in **P2** rather than the *-ortho* position in **P3**. Additionally, the latter complex also contained a bromide group at the *-meta* position. Meanwhile, the presence of a methoxy group at the *-meta* position in **P6** caused a higher SI value of 0.393 than that of **P3**. Based on the results of previous studies, the insertion of methyl [28] and hydroxyl [29-30] groups into the compounds enhanced the antiplasmodial activity. Nonetheless, it remained uncertain for the role of each functional group in improving the selectivity of the silver complexes.

Antiproliferative Activities

Transition metals like silver have long been known to be antimicrobial agents. However, there is still much to be discovered concerning its ability to act as an anticancer agent [31-32], even though there are reports that silver has anticancer activity *in vitro* [33]. The advantage of silver is that its toxicity is lower than those of other metals like platinum (e.g., cisplatin) [34]. On another note, thiosemicarbazones have a wide range of antiproliferative activities on different tumor cell lines, apart from displaying the common features of all compounds with carcinogenic potencies [35-36]. Meanwhile, silver phosphine has been shown to exert *in vitro* antiproliferative effects [37-38]. Based on the IC_{50} values, complexes **P2**, **P3**, **P4**, **P5**, and **P6** exerted modest antiproliferative effects on the human breast cancer MCF-7 and colon cancer HT-29 cell lines (Table 2). However, **P1** had the weakest antiproliferative potential in all cancer cell lines tested. However, as for the MDA-MB-231 carcinoma cancer cell line, good antiproliferative effects were also observed for **P2**, **P4**, and **P5**. This might be due to the hydroxyl group's presence [39] in P2 and the indolic group of **P4** and **P5**. Therefore, more in-depth studies are warranted concerning the roles of these silver compounds as metallotherapeutic drugs for cancers.

Table 2. Antiproliferative activities of silver complexes **1–6** (IC50 in μM)

Complexes	MDA-MB-231	HT-29	MCF-7
P1	15.11 ± 4.24	-	19.62 ± 4.87
P2	6.81 ± 1.69	7.23 ± 0.10	4.48 ± 0.86
P3	-	6.86 ± 0.17	3.51 ± 1.13
P4	5.48 ± 1.16	5.79 ± 1.92	7.13 ± 0.71
P5	5.27 ± 1.44	6.03 ± 0.76	4.34 ± 1.69
P6	-	7.14 ± 0.76	4.39 ± 0.74

■ **CONCLUSION**

Six silver complexes containing mixed ligands (4-phenyl-3-thiosemicarbazone derivatives and triphenylphosphine) have been successfully synthesized. The silver complexes were found to be dinuclear with tetrahedral geometry supported by the spectroscopic data discussed in the earlier section. Antiproliferative activities were investigated using MCF-7 breast and MDA-MB-231 carcinoma cancer cell lines and the HT-29 colon cancer cell line. Compounds **P2**-**P6** were worthy of in-depth studies as metallotherapeutic agents as their result exerted modest antiplasmodial activity against most cancer cells tested. On another note, all the compounds mentioned above had good activity against chloroquine-resistant *P. falciparum* parasites, but they were not as selective as conventional drugs. Consequently, modifications of the structural frame of 4-phenyl-3-thiosemicarbazone could improve the SI value of the resulting compound.

■ **AUTHOR CONTRIBUTIONS**

The project was conceived by Rozie Sarip and Nor Fadilah Rajab. Chemical synthesis and characterizations were performed mainly by Nur Adila Fatin Mohd Khir with the help of Nur Rahimah Fitrah Mohd Sofyan. In-vitro studies of the antiplasmodial and antiproliferative activity were done by Mohd Ridzuan Mohd Abd Razak and Fariza Juliana Nordin, respectively. The manuscript

was written by Nur Adila Fatin Mohd Khir, Mohd Ridzuan Mohd Abd Razak, Fariza Juliana Nordin, and Rozie Sarip.

■ **REFERENCES**

[1] Chen, J.J., Gan, Z.L., Huang, Q., and Yi, X.Y., 2017, Well-defined dinuclear silver phosphine complexes based on nitrogen donor ligand and their high efficient catalysis for A^3-coupling reaction, *Inorg. Chim. Acta*, 466, 93–99.

[2] Papanikolaou, P.A., Papadopoulos, A.G., Andreadou, E.G., Hatzidimitriou, A., Cox, P.J., Pantazaki, A.A., and Aslanidis, P., 2015, The structural and electronic impact on the photophysical and biological properties of a series of Cu^I and Ag^I complexes with triphenylphosphine and pyrimidine-type thiones, *New J. Chem.*, 39 (6), 4830–4844.

[3] Engelbrecht, Z., Meijboom, R., and Cronjé, M.J., 2018, The ability of silver(I) thiocyanate 4-methoxyphenyl phosphine to induce apoptotic cell death in esophageal cancer cells is correlated to mitochondrial perturbations, *BioMetals*, 31 (2), 189–202.

[4] Human, Z., Munyaneza, A., Omondi, B., Sanabria, N.M., Meijboom, R., and Cronjé, M.J., 2014, The induction of cell death by phosphine silver(I) thiocyanate complexes in SNO-esophageal cancer cells, *BioMetals*, 28 (1), 219–228.

[5] Chaves, J.D.S., Neumann, F., Francisco, T.M., Corrêa, C.C., Lopes, M.T.P., Silva, H., Fontes, A.P.S., and de Almeida, M.V., 2014, Synthesis and cytotoxic activity of gold(I) complexes containing phosphines and 3-benzyl-1,3-thiazolidine-2-thione or 5-phenyl-1,3,4-oxadiazole-2-thione as ligands, *Inorg. Chim. Acta*, 414, 85–90.

[6] Adams, M., Barnard, L., de Kock, C., Smith, P.J., Wiesner, L., Chibale, K., and Smith, G.S., 2016, Cyclopalladated organosilane-tethered thiosemicarbazones: Novel strategies for improving anti-plasmodial activity, *Dalton Trans.*, 45 (13), 5514–5520.

[7] Haas, K.L., and Franz, K.J., 2009, Application of metal coordination chemistry to explore and manipulate cell biology, *Chem. Rev.*, 109 (10), 4921–4960.

[8] Viñuelas-Zahínos, E., Luna-Giles, F., Torres-Garcia, P., and Fernández-Calderón, M.C., 2011, Co(III), Ni(II), Zn(II) and Cd(II) complexes with 2-acetyl-2-thiazoline thiosemicarbazone: Synthesis, characterization, X-ray structures and antibacterial activity, *Eur. J. Med. Chem.*, 46 (1), 150–159.

[9] Mustafa, A.Z.A., Altaf, M., Monim-ul-Mehboob, M., Fettouhi, M., Wazeer, M.I.M., Isab, A.A., Dhuna, V., Bhatia, G., and Dhuna, K., 2014, Tetrakis(1-3-diazinane-2-thione)platinum(II) chloride monohydrate complex: Synthesis, spectroscopic characterization, crystal structure and *in vitro* cytotoxic activity against A549, MCF7, HCT15 and HeLa human cancer lines, *Inorg. Chem. Commun.*, 44, 159–163.

[10] Netalkar, P.P., Netalkar, S.P., and Revankar, V.K., 2014, Nickel(II) complexes of thiosemicarbazones: synthesis, characterization, X-ray crystallographic studies and in vitro antitubercular and antimicrobial studies, *Transition Met. Chem.*, 39 (5), 519–526.

[11] Shahsavani, E., Khalaji, A.D., Feizi, N., Kučeráková, M., and Dušek, M., 2015, Synthesis, characterization, crystal structure and antibacterial activity of new sulfur-bridged dinuclear silver(I) thiosemicarbazone complex [Ag$_2$(PPh$_3$)$_2$(μ-S-Brcatsc)$_2$(η^1-S-Brcatsc)$_2$](NO$_3$)$_2$, *Inorg. Chim. Acta*, 429, 61–66.

[12] Hemmert, C., Fabié, A., Fabre, A., Benoit-Vical, F., and Gornitzka, H., 2013, Synthesis, structures, and antimalarial activities of some silver(I), gold(I) and gold(III) complexes involving *N*-heterocyclic carbene ligands, *Eur. J. Med. Chem.*, 60, 64–75.

[13] Isab, A.A., Nawaz, S., Saleem, M., Altaf, M., Monim-ul-Mehboob, M., Ahmad, S., and Evans, H.S., 2010, Synthesis, characterization and antimicrobial studies of mixed ligand silver(I) complexes of thioureas and triphenylphosphine; crystal structure of {[Ag(PPh$_3$)(thiourea)(NO$_3$)]$_2$·[Ag(PPh$_3$)(thiourea)]$_2$(NO$_3$)$_2$}, *Polyhedron*, 29 (4), 1251–1256.

586

Indones. J. Chem., 2021, 21 (3), 575 - 587

[14] Chaves, J.D.S., Tunes, L.G., de J. Franco, C.H., Francisco, T.M., Corrêa, C.C., Murta, S.M.F., Monte-Neto, R.L., Silva, H., Fontes, A.P., and de Almeida, M.V., 2017, Novel gold(I) complexes with 5-phenyl-1,3,4-oxadiazole-2-thione and phosphine as potential anticancer and antileishmanial agents, *Eur. J. Med. Chem.*, 127, 727–739.

[15] Benmohammed, A., Khoumeri, O., Djafri, A., Terme, T., and Vanelle, P., 2014, Synthesis of novel highly functionalized 4-thiazolidinone derivatives from 4-phenyl-3-thiosemicarbazones, *Molecules*, 19 (3), 3068–3083.

[16] Noedl, H., Bronnert, J., Yingyuen, K., Attlmayr, B., Kollaritsch, H., and Fukuda, M., 2005, Simple histidine-rich protein 2 double-site sandwich enzyme-linked immunosorbent assay for use in malaria drug sensitivity testing, *Antimicrob. Agents Chemother.*, 49 (8), 3575–3577.

[17] Noedl, H., Wernsdorfer, W.H., Miller, R.S., and Wongsrichanalai, C., 2002, Histidine-rich protein II: A novel approach to malaria drug sensitivity testing, *Antimicrob. Agents Chemother.*, 46 (6), 1658–1664.

[18] Mohd Abd Razak, M.R., Afzan, A., Ali, R., Amir Jalaluddin, N.F., Wasiman, M.I., Shiekh Zahari, S.H., Abdullah, N.R., and Ismail, Z., 2014, Effect of selected local medicinal plants on the asexual blood stage of chloroquine resistant *Plasmodium falciparum*, *BMC Complementary Altern. Med.*, 14 (1), 492.

[19] Noedl, H., Wernsdorfer, W.H., Kollaritsch, H., Looareesuwan, S., Miller, R.S., and Wongsrichanalai, C., 2003, Malaria drug-susceptibility testing. HRP2-based assays: current data, future perspectives, *Wien. Klin. Wochenschr.*, 115 (Suppl. 3), 23–27.

[20] Mosmann, T., 1983, Rapid colorimetric assay for cellular growth and survival: Application to proliferation and cytotoxicity assays, *J. Immunol. Methods*, 65 (1-2), 55–63.

[21] Vichai, V., and Kirtikara, K., 2006, Sulforhodamine B colorimetric assay for cytotoxicity screening, *Nat. Protocols*, 1 (3), 1112–1116.

[22] Altaf, M., Stoeckli-Evans, H., Cuin, A., Sato, D.N., Pavan, F.R., Leite, C.Q.F., Ahmad, S., Bouakka, M., Mimouni, M., Khardli, F.Z., and Hadda, T.B., 2013, Synthesis, crystal structures, antimicrobial, antifungal and antituberculosis activities of mixed ligand silver(I) complexes, *Polyhedron*, 62, 138–147.

[23] Sultana, R., Lobana, T.S., Sharma, R., Castineiras, A., Akitsu, T., Yahagi, K., and Aritake, Y., 2010, Heterocyclic thioamide derivatives of coinage metals (Cu, Ag): Synthesis, structures and spectroscopy, *Inorg. Chim. Acta*, 363 (13), 3432–3441.

[24] Sharma, R., Lobana, T.S., Kaur, M., Thathai, N., Hundal, G., Jasinski, J.P., and Butcher, R.J., 2016, Variable coordinating activity of sulfur in silver(I) complexes with thiophene based N-1-substituted thiosemicarbazones: First case of thiopheneyl-thione sulfur bridging in a dinuclear complex, *J. Chem. Sci.*, 128 (7), 1103–1112.

[25] Nawaz, S., Isab, A.A., Merz, K., Vasylyeva, V., Metzler-Nolte, N., Saleem, M., and Ahmad, S., 2011, Synthesis, characterization and antimicrobial studies of mixed ligand silver(I) complexes of triphenylphosphine and heterocyclic thiones: Crystal structure of bis[{(μ²-diazinane-2-thione)(diazinane-2-thione)(triphenylphosphine)silver(I) nitrate}], *Polyhedron*, 30 (9), 1502–1506.

[26] Venkatachalam, T.K., Pierens, G.K., Bernhardt, P.V., Stimson, D.H.R., Bhalla, R., Lambert, L., and Reutens, D.C., 2016, Heteronuclear NMR spectroscopic investigations of gallium complexes of substituted thiosemicarbazones including X-ray crystal structure, a new halogen exchange strategy, and ^{18}F radiolabelling, *Aust. J. Chem.*, 69 (9), 1033–1048.

[27] Waiganjo, B., Moriasi, G., Onyancha, J., Elias, N., and Muregi, F., 2020, Antiplasmodial and cytotoxic activities of extracts of selected medicinal plants used to treat malaria in Embu county, Kenya, *J. Parasitol. Res.*, 2020, 8871375.

[28] Souza, M.C., Padua, T.A., Torres, N.D., Costa, M.F.S., Facchinetti, V., Gomes, C.R.B., Souza, M.V.N., and Henriques, M.G., 2015, Study of the antimalarial properties of hydroxyethylamine derivatives using green fluorescent protein transformed *Plasmodium berghei*, *Mem. Inst. Oswaldo Cruz*, 110 (4), 560–565.

[29] Loginova, N.V., Koval'chuk, T.V., Gres, A.T., Osipovich, N.P., Polozov, G.I., Halauko, Y.S., Faletrov, Y.V., Harbatsevich, H.I., Hlushko, A.V., Azarko, I.I., and Bokshits, Y.V., 2015, Redox-active metal complexes of sterically hindered phenolic ligands: Antibacterial activity and reduction of cytochrome c. Part IV. Silver(I) complexes with hydrazone and thiosemicarbazone derivatives of 4,6-di-*tert*-butyl-2,3-dihydroxybenzaldehyde, *Polyhedron*, 88, 125–137.

[30] Wani, W.A., Jameel, E., Baig, U., Mumtazuddin, S., and Hun, L.T., 2015, Ferroquine and its derivatives: New generation of antimalarial agents, *Eur. J. Med. Chem.*, 101, 534–551.

[31] Medici, S., Peana, M., Nurchi, V.M., Lachowicz, J.I., Crisponi, G., and Zoroddu, M.A., 2015, Noble metals in medicine: Latest advances, *Coord. Chem. Rev.*, 284, 329–350.

[32] Banti, C.N., and Hadjikakou, S.K., 2013, Anti-proliferative and anti-tumor activity of silver(I) compounds, *Metallomics*, 5 (6), 569–596.

[33] Majeed, S., Abdullah, M.S., Nanda, A., and Ansari, M.T., 2016, In vitro study of the antibacterial and anticancer activities of silver nanoparticles synthesized from *Penicillium brevicompactum* (MTCC-1999), *J. Taibah Univ. Sci.*, 10 (4), 614–620.

[34] Ndagi, U., Mhlongo, N., and Soliman, M.E., 2017, Metal complexes in cancer therapy - an update from drug design perspective, *Drug Des., Dev. Ther.*, 11, 599–616.

[35] Arora, S., Agarwal, S., and Singhal, S., 2014, Anticancer activities of thiosemicarbazides/thio semicarbazones: A review, *Int. J. Pharm. Pharm. Sci.*, 6 (9), 34–41.

[36] Serda, M., Kalinowski, D.S., Rasko, N., Potůčková, E., Mrozek-Wilczkiewicz, A., Musiol, R., Małecki, J.G., Sajewicz, M., Ratuszna, A., Muchowicz, A., Gołąb, J., Šimůnek, T., Richardson, D.R., and Polanski, J., 2014, Exploring the anti-cancer activity of novel thiosemicarbazones generated through the combination of retro-fragments: Dissection of critical structure-activity relationships, *Plos One*, 9 (10), e110291.

[37] Human-Engelbrecht, Z., Meijboom, R., and Cronjé, M.J., 2017, Apoptosis-inducing ability of silver(I) cyanide-phosphines useful for anti-cancer studies, *Cytotechnology*, 69 (4), 591–600.

[38] Kyros, L., Kourkoumelis, N., Kubicki, M., Male, L., Hursthouse, M.B., Verginadis, I.I., Gouma, E., Karkabounas, S., Charalabopoulos, K., and Hadjikakou, S.K., 2010, Structural properties, cytotoxicity, and anti-inflammatory activity of silver(I) complexes with tris(*p*-tolyl)phosphine and 5-chloro-2-mercaptobenzothiazole, *Bioinorg. Chem. Appl.*, 2010, 386860.

[39] Abdul Halim, S.N.A., Nordin, F.J., Mohd Abd Razak, M.R., Mohd Sofyan, N.R.F., Abdul Halim, S.N., Rajab, N.F., and Sarip, R., 2019, Synthesis, characterization, and evaluation of silver(I) complexes with mixed-ligands of thiosemicarbazones and diphenyl(*p*-tolyl)phosphine as biological agents, *J. Coord. Chem.*, 72 (5-7), 879–893.